ACS Macro Letters

pubs.acs.org/macroletters Letter

Rapid Processing of Bottlebrush Coatings through UV-Induced Cross-Linking

Hao Mei, Adeline Huizhen Mah, Zhiqi Hu, Yilin Li, Tanguy Terlier, Gila E. Stein,* and Rafael Verduzco*

Cite This: ACS Macro Lett. 2020, 9, 1135−1142 Read Online

ACCESS | Metrics & More | Article Recommendations | Supporting Information

ABSTRACT: Bottlebrush polymers can be used to introduce novel surface properties including hydrophilicity, stimuli-responsiveness, and reduced friction forces. However, simple, general, and efficient approaches to cross-linking bottlebrush polymer films and coatings are limited. Here, we report that bottlebrush polymers with an unsaturated polynorbornene backbone and thiol-terminated side chains can be cross-linked on demand by UV irradiation to produce uniform and insoluble bottlebrush polymer coatings. To quantify the kinetics and efficiency of cross-linking by UV exposure (254 nm), we measured the normalized residual thickness (NRT) of bottlebrush and linear polymer films after UV exposure and solvent washing. For bottlebrush polymers with thiol-terminated polystyrene (PS) side chains, the NRT exceeded 60% for a UV dose of 1.0 J/cm^2, while unfunctionalized linear PS required a dose of 7.9 J/cm^2 to achieve similar NRT values. Rapid UV-induced cross-linking of the bottlebrush PS was attributed to the thiol−ene coupling of the thiol-terminated side chains with the unsaturated polynorbornene backbones, as demonstrated through FTIR measurements and control studies involving bottlebrush polymers with saturated backbones. To establish the broader applicability of this approach, UV-induced cross-linking was demonstrated for thin films of bottlebrush polymers with thiol-terminated poly(methyl acrylate) (BB-PMMA-SH) side chains and those with poly(ethylene glycol) (BB-PEG) and poly(lactic acid) (BB-PLA) side chains which do not contain thiol end groups. UV-induced cross-linking of BB-PEG and BB-PLA films required the use of a multifunctional thiol additive. Finally, we demonstrated that bottlebrush polymer multilayers can be fabricated through sequential deposition and UV-induced cross-linking of different bottlebrush polymer chemistries. The cross-linking process outlined in this work is simple, general, and efficient and produces solvent-resistant coatings that preserve the unique properties and functions of bottlebrush polymers.

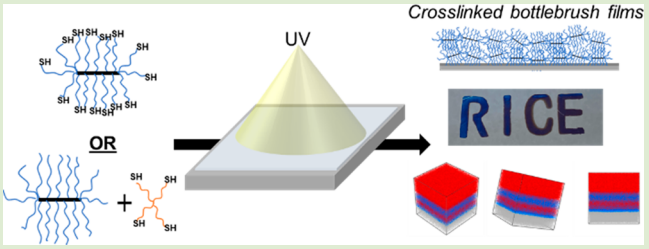

Bottlebrush polymers have a number of unique properties that make them attractive for modifying surfaces and interfaces. Various side-chain and side-chain end-group chemistries can be incorporated to deliver a desired property or functionality, and two (or more) types of side chains can be incorporated into a single bottlebrush polymer[1,2] to produce stimuli-responsive surfaces[3,4] or drive self-assembly into well-defined nanoscale patterns.[5] Furthermore, bottlebrush polymers have unique tribological properties, enabling their use to tailor frictional forces at solid/liquid interfaces.[6,7] Other potential applications rely on the dense, brush-like conformation of the side chains, which can be used to generate antifouling surfaces[8,9] and low-energy surfaces.[10,11]

Cross-linking can be used to improve the stability and robustness of polymer coatings and films. Cross-linking can help with adhesion to a surface, inhibit dissolution, and enable the sequential deposition of multiple polymer coatings.[12,13] However, simple, general, and efficient approaches to cross-linking bottlebrush polymer films and coatings are limited. While a number of prior studies have reported cross-linking of bottlebrush polymers, these prior studies have not focused on films and coatings and in many cases are based on a specific side-chain chemistry.[14−22] For example, bottlebrush polymers containing polyacrylonitrile segments in the side chains can be thermally cross-linked,[14] and metal-free click chemistry can be used to cross-link bottlebrush polymers containing azide functional groups in the side chains.[15] A series of studies utilized additives with thiol functional groups to cross-link liquid crystal brush block polymers via thiol−ene coupling between the additive and unsaturated bottlebrush backbone. This was implemented to fabricate self-assembled, nanoporous membranes.[16−19] In another recent study, a universal strategy to cross-link bottlebrush polymers in the bulk under UV light utilized miscible bisbenzophenone additives. This strategy was implemented to fabricate super sensitive touch sensors based on bottlebrush networks.[20,21] A recent study that focused on

Received: May 18, 2020
Accepted: July 17, 2020
Published: July 22, 2020

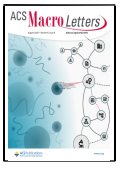

bottlebrush films showed that bottlebrush polymers with polystyrene (PS) side chains could be cross-linked through exposure to ionizing radiation.[22]

"Grafting-through" synthesis is a popular approach for bottlebrush polymer synthesis that incorporates reactive groups in the bottlebrush backbone and side chains. For example, ring-opening metathesis polymerization (ROMP) of norbornenyl-terminated macromonomers produces bottlebrush polymers with an unsaturated polynorbornene backbone.[1,23,24] A number of prior studies have reported the modification or cross-linking of some ROMP-derived polymers through thiol−ene reactions.[25−28] Furthermore, some controlled radical polymerization techniques allow the side chains to contain functional end groups during the macromonomer synthesis. For example, macromonomers produced through reversible addition−fragmentation chain transfer (RAFT) contain a fragment of the chain transfer agent (CTA) at the end of the chain that can be reduced to a thiol.[29−31] Macromonomers synthesized through atom transfer radical polymerization (ATRP) also enable the side chains to contain reactive end groups.[2,32−34]

Here, we investigated UV-induced thiol−ene coupling reactions for cross-linking films of ROMP-derived bottlebrush polymers, which contained an unsaturated polynorbornene backbone. Although thiol−ene coupling has been reported as a method to cross-link bottlebrush polymers, these prior studies focused on the cross-linking of bulk bottlebrush samples for the fabrication of free-standing membranes, which required several hours of UV exposure.[17,18] Here, we studied UV-induced cross-linking of bottlebrush films which could be cross-linked in minutes. We also varied the composition of the side chains to understand the generality of the approach. To quantify cross-linking, we studied thin films of bottlebrush polymers deposited on a surface and measured the normalized residual thickness (NRT = h/h_o) of the film after UV irradiation and solvent wash, where h_o was the initial film thickness and h the final film thickness after UV irradiation and solvent wash. We analyzed a series of bottlebrush polymers and studied the effects of initial film thickness, UV dose, side-chain length, side-chain chemistry, and end-group functionality on the NRT. The results presented below demonstrated that UV-induced thiol−ene coupling reactions provide a general approach for cross-linking bottlebrush films into solvent-resistant networks for a variety of side-chain chemistries.

We hypothesized that bottlebrush polymers containing an unsaturated polynorbornene backbone could be cross-linked through UV-induced radical thiol−ene coupling reactions if the polymers contained thiol-terminated side chains or were mixed with a multifunctional thiol-terminated additive. In the case of bottlebrush polymers with thiol-terminated side chains, we expected that cross-linking could occur without any additional reagents or additives. As for bottlebrush polymers without thiol-terminated side chains, the cross-linking could occur by adding a multifunctional thiol-terminated additive. These two cases are shown schematically in Scheme 1a, and a representative cross-linking mechanism is shown in Scheme 1b. To test these hypotheses, we produced a series of bottlebrush polymers using the "grafting-through" ROMP synthesis strategy.[1,2] The bottlebrushes all contained unsaturated polynorbornene backbones but differed in the chemistry and end-group functionality of side chains. We synthesized bottlebrush polymers with polystyrene (PS), poly(methyl methacrylate) (PMMA), polylactic acid (PLA), and poly-

Scheme 1. Overview of Bottlebrush Polymer Cross-Linking through UV-Induced Radical Thiol−Ene Coupling[a]

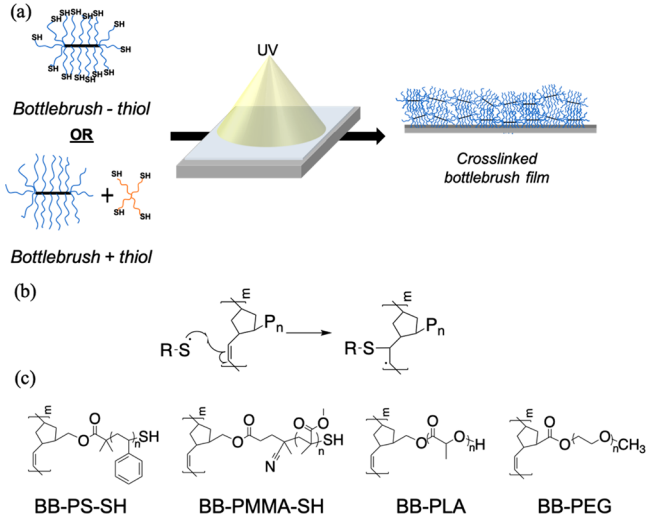

[a](a) Schematic illustration for cross-linking of bottlebrush films under UV light through thiol−ene coupling. (b) Proposed reaction scheme for bottlebrush film cross-linking via radical thiol−ene coupling. P_n represents the bottlebrush polymer side chain and R-S● represents a thiol radical, where the R group can be either a bottlebrush polymer or a small molecular additive. (c) Chemical structures for the bottlebrush polymers used in this study.

ethylene glycol (PEG) side chains. The structures of these polymers are shown in Scheme 1c. The PS and PMMA bottlebrush polymers contained thiol-terminated side chains, while the side chains of the PLA and PEG bottlebrush polymers were terminated by hydroxyl and methoxyl groups, respectively. In the case of PS bottlebrush polymers, we studied two side-chain molecular weights (approximately 3 and 6 kg/mol) and two backbone degrees of polymerization (DPs) for each side-chain molecular weight (entries 3 and 5−7 in Table 1). As control studies, we analyzed the cross-linking of unfunctionalized linear PS (L-PS) (entry 1 in Table 1) and a PS bottlebrush with a saturated backbone (entry 4 in Table 1). With the exception of L-PS which was acquired commercially, the synthesis of these materials was carried out using methods previously reported.[29,35−38] The characteristics of all the polymers prepared for this study are shown in Table 1. The naming convention for bottlebrush polymers used in this study includes the side-chain chemistry, side-chain molecular weight, and backbone degree of polymerization in the sample name. For example, BB-PS-SH-3k-20 denotes a bottlebrush polymer with thiol-terminated PS side chains of approximately 3 kg/mol and a backbone with 20 repeat units. The synthetic details of polymers used in this study are provided in the Supporting Information, including proton nuclear magnetic resonance (^{1}H NMR) spectroscopic analysis (Supporting Information Figures S1 and S2), gel permeation chromatography (GPC) analysis of macromonomers and bottlebrush polymers (Supporting Information Figures S3−S8), and additional chemical structures (Supporting Information Scheme S1).

We first analyzed the UV-induced cross-linking of L-PS and BB-PS-SH-3k-20. Films of each polymer were prepared by flow-coating onto precleaned silicon wafers and then exposed to UV light (254 nm, 3.3 mW/cm^2) in air. The UV dose was controlled by the exposure time. No other reagent or photoinitiator was included in the film. After exposure to UV

https://dx.doi.org/10.1021/acsmacrolett.0c00384
ACS Macro Lett. 2020, 9, 1135−1142

Table 1. Characteristics of Polymers Used in This Study[a]

entry	polymer[a]	side-chain molecular weight[b] (kg/mol)	overall M_w[c] (kg/mol)	backbone DP	$Đ$	conversion[d]
1	L-PS (linear)	--	192	--	--	N/A
2	L-CTA	0.5	32	67	1.10	N/A
3	BB-PS-SH-3k-20	2.6	42	16	1.27	92%
4	H-BB-PS-SH-3k-20	2.6	42	16	1.39	95%
5	BB-PS-SH-3k-150	2.6	400	152	1.44	97%
6	BB-PS-SH-6k-7	5.5	39	7	1.27	88%
7	BB-PS-SH-6k-80	5.5	420	77	1.73	97%
8	BB-PMMA-SH-4k-40	4.1	170	40	1.25	97%
9	BB-PEG-2k-30	2.1	61	29	1.12	98%
10	BB-PLA-3k-50	3.1	160	50	1.26	95%

[a]'L' denotes linear polymer, "BB" denotes bottlebrush, and "H-BB" denotes bottlebrush with a saturated backbone. PS = polystyrene, PEG = poly(ethylene glycol), PLA = poly(lactic acid), PMMA = poly(methyl methacrylate). $Đ$ denotes the molecular weight dispersity of the polymer, and conversion denotes the percentage of macromonomer incorporated in the final bottlebrush material based on GPC-RI analysis. [b]Measured by ^{1}H NMR. [c]Measured by GPC with multiangle laser light scattering detectors. [d]Estimated based on GPC-RI analysis.

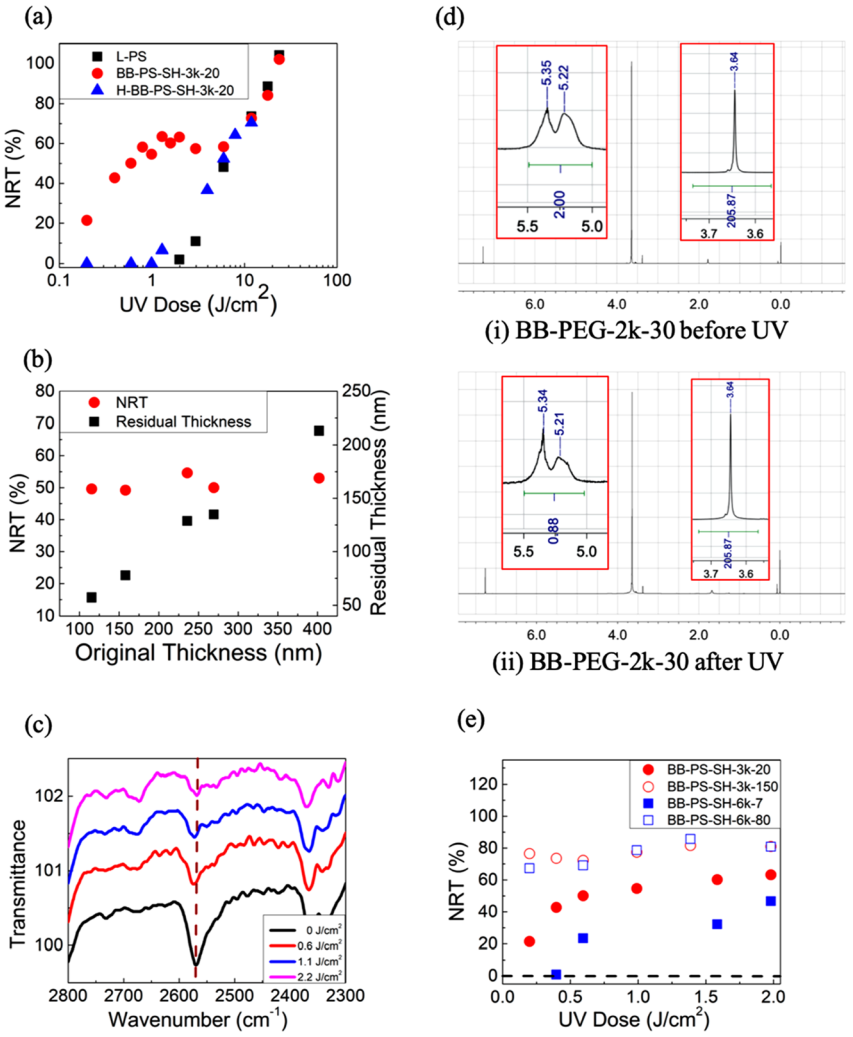

Figure 1. (a) Plot of the NRT as a function of UV dose for L-PS, BB-PS-SH-3k-20, and H-BB-PS-SH-3k-20 films under UV radiation. (b) NRT and residual thickness of BB-PS-SH-3k-20 after UV radiation at a dose of 1.6 J/cm^2. (c) FTIR spectra for L-CTA and PETMP at varying UV doses. (d) ^{1}H NMR spectra for BB-PEG-2k-30 before and after UV irradiation (dose = 23.8 J/cm^2). (e) NRT for BB-PS-SH with different side-chain lengths and backbone DPs with different UV dose. The wavelength of the UV light was 254 nm.

light, the films were immersed in tetrahydrofuran (THF) to remove un-cross-linked polymer, and the film thicknesses were measured and compared to the initial film thicknesses. We defined the normalized residual thickness (NRT = h/h_o) as the ratio of the final film thickness h after UV-induced cross-linking and THF wash to the initial film thickness h_o. A higher NRT indicated a higher degree of cross-linking of the bottlebrush film, and an NRT of 100% corresponded to a fully cross-linked film. As shown in Figure 1a, the NRT for BB-PS-SH-3k-20 films increased rapidly under UV exposure, from

https://dx.doi.org/10.1021/acsmacrolett.0c00384
ACS Macro Lett. 2020, 9, 1135−1142

an NRT of 0 to 60% with doses in the range of 0−1.0 J/cm^2. By comparison, the NRT for L-PS films was approximately 0% with a dose of 1.0 J/cm^2 and did not reach 60% NRT until a much higher dose of 7.9 J/cm^2. With doses of 11.9 J/cm^2 and greater, the NRT for films of L-PS and BB-PS-SH-3k-20 were similar and continued to increase with UV dose. The UV-induced cross-linking of L-PS has been extensively studied, and the mechanism for the UV-induced cross-linking of L-PS in air involves dissociation of C−H bonds to produce radicals followed by oxidation and bridging between chains. A schematic for this cross-linking mechanism is shown in the Supporting Information Scheme S2.[39−42] Similar experiments using longer wavelengths of UV irradiation (365 nm) did not produce any measurable cross-linking of L-PS nor BB-PS-SH-3k-20.

We also studied the UV-induced cross-linking of PS bottlebrush polymers with a saturated backbone (H-BB-PS-SH-3k-20). To synthesize these materials, the backbone of BB-PS-SH-3k-20 was reduced using *p*-toluenesulfonyl hydrazide and *N*,*N*-diisopropyl-ethylamine in xylenes.[43] A detailed description is provided in the Supporting Information, and the ^{1}H NMR spectra for BB-PS-SH-3k-20 and H-BB-PS-SH-3k-20 are shown in the Supporting Information Figure S9. Films of H-BB-PS-SH-3k-20 exposed to UV light (254 nm) cross-linked slowly with increasing UV dose, following a trend very similar to that of L-PS, as shown in Figure 1a. This indicated similar cross-linking mechanisms for H-BB-PS-SH-3k-20 and L-PS.

To further understand the UV-induced cross-linking of BB-PS-SH films, we analyzed the effects of film thickness, UV dose, side-chain length, and bottlebrush molecular weight. BB-PS-SH-3k-20 films ranging from 100 to 400 nm in thickness were prepared and exposed to UV radiation at a dose of 1.6 J/cm^2. These film thicknesses were much smaller than the penetration depth l ($l \approx 350$ μm) of UV light (254 nm).[44] As shown in Figure 1b, the NRT was nearly independent of film thickness, and all films had an NRT of approximately 55% after a UV dose of 1.6 J/cm^2.

The NRT measurements shown in Figure 1a show that PS bottlebrush polymers with thiol end groups and unsaturated backbones cross-linked rapidly under UV light, while linear PS polymers or PS bottlebrush polymers with saturated backbones required a much higher UV dose. To obtain direct evidence for the radical thiol−ene coupling reaction for bottlebrush polymers, we attempted *in situ* FTIR analysis of the bottlebrush films during cross-linking, but these failed likely due to the low concentration of thiol and carbon−carbon double bonds in the film. For example, the mass fraction of thiol functional groups in BB-PS-SH-3k-20 is around 1.2 wt %. As an alternative, we synthesized a bottlebrush polymer with short side chains: a polynorbornene polymer with pendant chain transfer agent (CTA), denoted L-CTA (see Supporting Information Scheme S1). This polymer was blended with a multifunctional thiol reagent, pentaerythritol tetrakis(3-mercaptopropionate) (PETMP, Scheme 1c), and studied by *in situ* FTIR analysis under UV radiation. PETMP was added to the film at a 1:1 molar ratio of thiol to carbon−carbon double bonds in the polynorbornene backbone. Under UV radiation, a clear reduction in the FTIR absorbance peak at 2570 cm^{-1} (S−H vibration) was observed in Figure 1c, which reflected the reaction of the thiols with the unsaturated polynorbornene backbone.[28,45] Control experiments involving irradiation of pure PETMP (Supporting Information Figure S10) or pure L-CTA did not produce any change in the FTIR spectra or measurable cross-linking, indicating that reaction only occurs when these two are blended.

In addition, we conducted ^{1}H NMR tests to obtain additional evidence for bottlebrush cross-linking through thiol−ene coupling by analyzing BB-PEG-2k-30 and BB-PS-SH-6k-80 and before and after exposure to UV irradiation (dose = 23.8 J/cm^2). ^{1}H NMR measurements can detect vinylic hydrogens from the unsaturated polynorbornene backbone, and the proposed thiol−ene coupling chemistry should be associated with a decrease in the corresponding peak intensity. A representative experiment involving BB-PEG-2k-30 both before and after UV-induced cross-linking is shown in Figure 1d. The backbone vinylic hydrogens have a chemical shift of approximately 5.3 and 5.2 ppm, and the integrated peak intensities were normalized with respect to the hydrogens on the PEG side chains, which have a chemical shift of approximately 3.6 ppm. After cross-linking, the integrated peak intensities at 5.3 and 5.2 ppm decreased by 56%, as shown in Figure 1d. This is a significant reduction in the peak intensity that demonstrates a reaction involving the unsaturated polynorbornene backbone. Similar measurements were performed with BB-PS-SH-6k-80 as described in the Supporting Information, and ^{1}H NMR analyses for these samples are provided in the Supporting Information Figure S11.

We also studied the effects of the side-chain molecular weight and the polymer molecular weight on cross-linking. We analyzed the cross-linking of four PS bottlebrush polymers: two had 3 kg/mol side chains (BB-PS-3k-20 and BB-PS-3k-150), and two had 6 kg/mol side chains (BB-PS-6k-7 and BB-PS-6k-80). The molecular weights of the shorter backbone (BB-PS-3K-20 and BB-PS-6K7) and longer backbone (BB-PS-3k-150 and BB-PS-6k-80) bottlebrushes were matched at approximately 40 and 400 kg/mol, respectively. Films of each polymer were deposited on a surface (with thicknesses of approximately 150 nm), exposed to UV light, and then washed and analyzed to measure NRT as a function of UV dose as shown in Figure 1e. The results showed that increasing the polymer molecular weight by increasing the backbone DP increased NRT for low exposure doses, as expected,[46] while the impact of the side-chain length was unclear. The NRT for BB-PS-6k-7 was lower than that for BB-PS-3k-20, while BB-PS-3k-150 and BB-PS-6k-80 exhibited similar NRT values over the range of UV doses tested.

To understand the broader applicability of cross-linking ROMP-derived bottlebrush polymers, we studied the UV-induced cross-linking of bottlebrushes with different side-chain chemistries: PMMA (BB-PMMA-SH-4k-40) (entry 8 in Table 1), PEG (BB-PEG-2k-30) (entry 9 in Table 1), and PLA (BB-PLA-3k-50) (entry 10 in Table 1). The PMMA side chains on BB-PMMA-SH-4k-40 were terminated by thiol groups, and films could be cross-linked by exposure to UV light without any additives. As shown in Figure 2a, at room temperature, we did not observe any cross-linking of BB-PMMA-SH-4k-40. At 105 °C, which is near the glass-transition temperature of PMMA, we observed significant cross-linking at UV doses greater than 2.0 J/cm^2 in air. For comparison, we also studied the UV-induced cross-linking of PS bottlebrush films (BB-PS-3k-20) at 100 °C and observed a more rapid increase of NRT followed by a decrease in NRT (as shown in the Supporting Information Figure S12), which suggests that the film degraded with higher UV doses at elevated temperatures.[47,48]

https://dx.doi.org/10.1021/acsmacrolett.0c00384
ACS Macro Lett. 2020, 9, 1135−1142

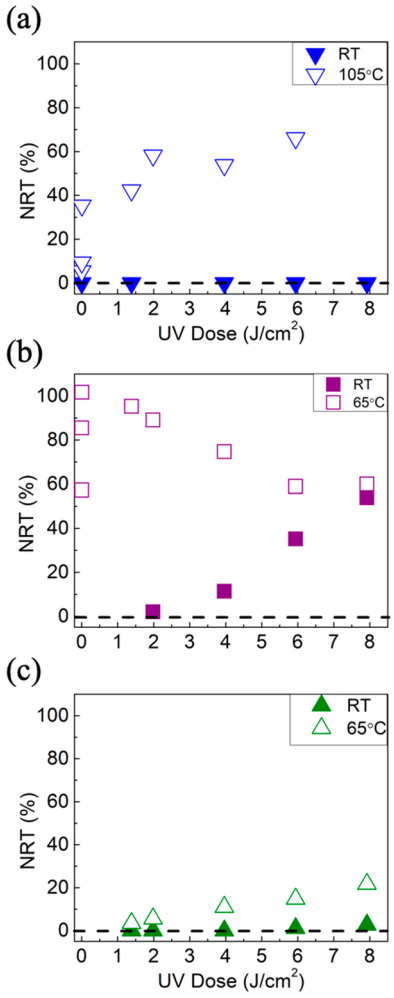

Figure 2. NRT as a function of UV dose for (a) BB-PMMA-SH-4k-40, (b) BB-PEG-2k-30 with PETMP, and (c) BB-PLA-3k-50 with PETMP at room temperature (RT) and at an elevated temperature.

In the case of BB-PEG-2k-30 and BB-PLA-3k-50, these materials did not contain terminal thiols, and we therefore added a multifunctional thiol reagent, PETMP, to achieve UV-induced cross-linking of thin films. PETMP was added at an equimolar ratio of thiols and carbon−carbon double bonds. These materials were studied at both ambient and elevated temperatures. Both materials exhibited very little cross-linking at ambient temperatures, but some cross-linking was observed for both materials at elevated temperatures (approximately 65 °C). The BB-PEG-2k-30 reached an NRT of approximately 60% under a UV dose of 2.0 J/cm^2, while BB-PLA-3k-50 reach a maximum NRT of only 20% for UV doses up to 7.9 J/cm^2. No cross-linking of either BB-PLA-3k-50 or BB-PEG-2k-30 was observed without the addition of PETMP, even at elevated temperatures. In addition, no cross-linking was observed for linear PEG with PETMP at similar conditions. The NRT results for all the polymers are summarized in Supporting Information Tables S1 and S2.

These results demonstrate that ROMP-derived bottlebrush polymers can be rapidly cross-linked under UV light. For PS and PMMA bottlebrush polymers with thiol-terminated side chains, cross-linking was achieved without the addition of any cross-linking reagent or photoinitiator. In the case of PLA and PEG bottlebrush polymers that did not contain thiol functional groups, an external thiol reagent (PETMP) was required to cross-link the films. However, the kinetics of film cross-linking varied significantly with side-chain chemistry. While all PS bottlebrushes studied could be cross-linked at ambient temperatures, PMMA bottlebrushes required elevated temperatures. Similarly, very different kinetics for UV-induced cross-linking was observed for BB-PEG-2k-30 and BB-PLA-3k-50, both of which required an added thiol-containing reagent for cross-linking. One potential source for the large differences in photo-cross-linking is the different effect UV exposure has on different polymer chemistries. As examples, PMMA[49] and PLA[50] undergo chain scission when exposed to ionizing radiation, while PS will cross-link[46] and poly(ethylene glycol)

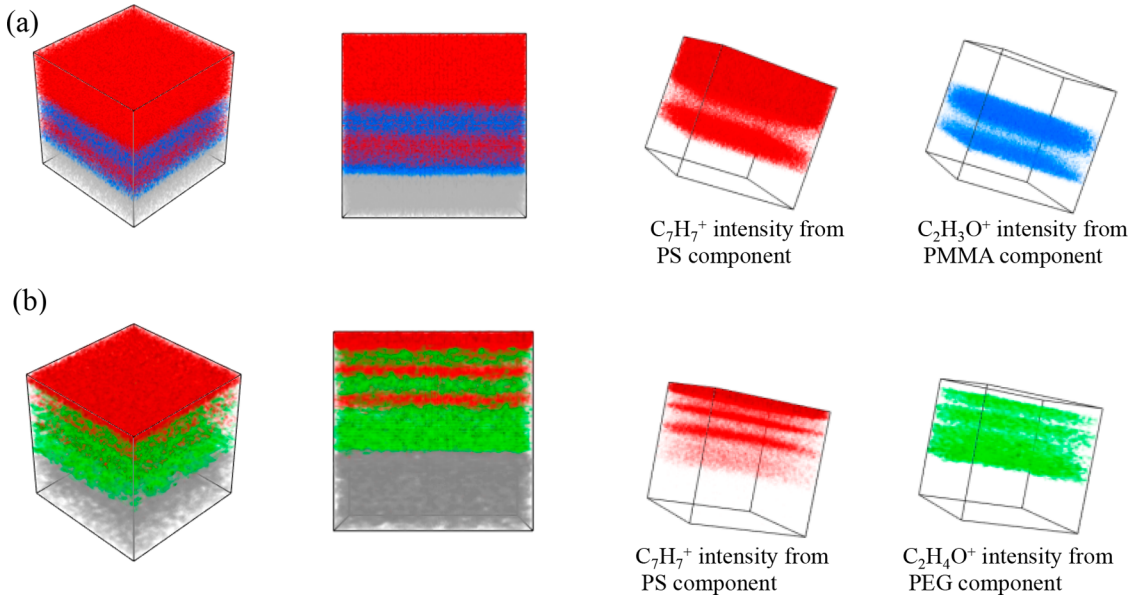

Figure 3. ToF-SIMS analyses of multilayer bottlebrush film coatings. (a) Three-dimensional false-color spectra for PS−PMMA multilayer coatings. Red indicates PS, blue PMMA, and gray the silicon wafer substrate. (b) Three-dimensional false-color spectra for PS−PEG multilayer coatings. Red indicates PS, green PEG, and gray the silicon wafer substrate.

https://dx.doi.org/10.1021/acsmacrolett.0c00384
ACS Macro Lett. 2020, 9, 1135−1142

(PEG) is stable under UV exposure.[51] As a result, for PLA and PMMA, photoinduced cross-linking will compete with photoinduced degradation and chain scission, resulting in slow and/or poor cross-linking. This is consistent with the trends we observed, in which PS bottlebrush films cross-link most readily, followed by PEG bottlebrushes and then PMMA and PLA. Another source of differing cross-linking kinetics is the use of multifunctional thiols for PEG and PLA bottlebrushes vs thiol-functionalized side chains in PS and PMMA bottlebrushes.

This work demonstrates a simple approach to produce cross-linked bottlebrush films with a variety of side-chain chemistries, and the method can be implemented to produce patterned films and/or multilayer coatings and films. To demonstrate patterning, we exposed bottlebrush thin films to UV radiation through a shadow mask. After washing in THF, only the exposed regions remained. A representative image of a patterned BB-PS-SH-3k-20 film on a silicon wafer is shown in the Supporting Information Figure S13. We also produced multilayer bottlebrush polymer films through sequential, alternating deposition and UV-induced cross-linking steps. In the first example, four alternating layers of PS (BB-PS-SH-3k-20) and PMMA (BB-PMMA-4k-40) bottlebrushes were deposited on a silicon wafer. Each layer was deposited by flow-coating from tetrahydrofuran (THF), exposed to UV light (2.0 J/cm^2) at room temperature and 105 °C, respectively, and immersed in THF to remove un-cross-linked material before deposition of the next layer. The final multilayer film was analyzed by depth profiling through time-of-flight secondary ion mass spectrometry (ToF-SIMS), and the results are shown in the three-dimensional false-color spectra in Figure 3a. These spectra show the formation of multilayer bottlebrush films. We similarly cast a six-layer film of alternating PS (BB-PS-SH-3k-20) and PEG (BB-PEG-2k-30) bottlebrush layers, and the ToF-SIMS depth profiling analyses are shown in Figure 3b. The BB-PS-SH-3k-20 and BB-PEG-2k-30 layers were cross-linked using a UV dose of 2.0 J/cm^2 at room temperature and 65 °C, respectively, and PETMP was added to the BB-PEG-2k-30 layer during casting.

In conclusion, we studied the UV-induced cross-linking of ROMP-derived bottlebrush polymer thin films. We found that films of PS bottlebrushes with unsaturated polynorbornene backbones and thiol-terminated side chains could be cross-linked under much lower UV doses (approximately 1.0 J/cm^2) relative to linear polystyrene films, which required much higher doses (7.9 J/cm^2) to achieve significant cross-linking (60% NRT or higher). Bottlebrush polymers with saturated backbones similarly required higher UV doses (7.9 J/cm^2) to achieve a significant degree of cross-linking (60% NRT or higher), demonstrating the importance of both thiol-terminated side chains and unsaturated polynorbornene backbones in the cross-linking reaction. FTIR and ^{1}H NMR results directly supported the proposed thiol−ene reaction mechanism. UV-induced cross-linking was also demonstrated for bottlebrushes with PMMA, PEG, and PLA side chains. For these chemistries, elevated temperatures (in the case of PMMA) and multifunctional thiol additives (in the cases of PEG and PLA) were required to produce cross-linked bottlebrush coatings. We found significant differences in cross-linking kinetics, which we attribute to degradation of some side-chain polymer chemistries under UV-irradiation, which can compete with cross-linking. This work demonstrates a general approach for cross-linking of bottlebrush polymers with unsaturated polynorbornene backbones, providing a simple route to produce patterned, solvent-resistant single layer, and multilayer bottlebrush polymer films.

■ ASSOCIATED CONTENT

Supporting Information

The Supporting Information is available free of charge at https://pubs.acs.org/doi/10.1021/acsmacrolett.0c00384.

Details on polymer synthesis and characterization, additional chemical structures, schematics for cross-linking mechanisms, additional FTIR, additional ^{1}H NMR spectra, additional *NRT* measurements for cross-linked films, and images of a cross-linked and patterned bottlebrush coating (PDF)

■ AUTHOR INFORMATION

Corresponding Authors

Rafael Verduzco − *Department of Chemical and Biomolecular Engineering, Nanosystems Engineering Research Center for Nanotechnology-Enabled Water Treatment, and Department of Materials Science and NanoEngineering, Rice University, Houston, Texas 77005, United States;* orcid.org/0000-0002-3649-3455; Email: rafaelv@rice.edu

Gila E. Stein − *Department of Chemical and Biomolecular Engineering, University of Tennessee, Knoxville, Tennessee 37996, United States;* orcid.org/0000-0002-3973-4496; Email: gstein4@utk.edu

Authors

Hao Mei − *Department of Chemical and Biomolecular Engineering and Nanosystems Engineering Research Center for Nanotechnology-Enabled Water Treatment, Rice University, Houston, Texas 77005, United States*

Adeline Huizhen Mah − *Department of Materials Science and Engineering, University of Houston, Houston, Texas 77004, United States*

Zhiqi Hu − *Department of Chemical and Biomolecular Engineering, Rice University, Houston, Texas 77005, United States*

Yilin Li − *Department of Chemical and Biomolecular Engineering, Rice University, Houston, Texas 77005, United States*

Tanguy Terlier − *SIMS Lab, Shared Equipment Authority, Rice University, Houston, Texas 77005, United States*

Complete contact information is available at: https://pubs.acs.org/10.1021/acsmacrolett.0c00384

Notes

The authors declare no competing financial interest.

■ ACKNOWLEDGMENTS

H.M., Z.H., Y.L., and R.V. acknowledge support from the Welch Foundation under Grant No. C-1888 and the National Science Foundation under Grant Nos. CMMI 1563008 and CMMI 1934045 and the NSF Nanosystems Engineering Research Center for Nanotechnology-Enabled Water Treatment (EEC 1449500). A.H.M. and G.E.S. acknowledge support by the National Science Foundation under Award No. CMMI 1727517. ToF-SIMS measurements were supported by the National Science Foundation under Grant No. CBET 1626418. ToF-SIMS analyses were carried out with support provided by the Shared Equipment Authority at Rice University.

REFERENCES

(1) Verduzco, R.; Li, X.; Pesek, S. L.; Stein, G. E. Structure, Function, Self-Assembly, and Applications of Bottlebrush Copolymers. *Chem. Soc. Rev.* **2015**, *44* (8), 2405−2420.

(2) Xie, G.; Martinez, M. R.; Olszewski, M.; Sheiko, S. S.; Matyjaszewski, K. Molecular Bottlebrushes as Novel Materials. *Biomacromolecules* **2019**, *20* (1), 27−54.

(3) Xu, B.; Feng, C.; Hu, J.; Shi, P.; Gu, G.; Wang, L.; Huang, X. Spin-Casting Polymer Brush Films for Stimuli-Responsive and Anti-Fouling Surfaces. *ACS Appl. Mater. Interfaces* **2016**, *8* (10), 6685−6692.

(4) Sowers, M. A.; McCombs, J. R.; Wang, Y.; Paletta, J. T.; Morton, S. W.; Dreaden, E. C.; Boska, M. D.; Ottaviani, M. F.; Hammond, P. T.; Rajca, A.; Johnson, J. A. Redox-Responsive Branched-Bottlebrush Polymers for *in Vivo* MRI and Fluorescence Imaging. *Nat. Commun.* **2014**, *5*, 5460.

(5) Fei, H.-F.; Li, W.; Bhardwaj, A.; Nuguri, S.; Ribbe, A.; Watkins, J. J. Ordered Nanoporous Carbons with Broadly Tunable Pore Size Using Bottlebrush Block Copolymer Templates. *J. Am. Chem. Soc.* **2019**, *141*, 17006.

(6) Banquy, X.; Burdyńska, J.; Lee, D. W.; Matyjaszewski, K.; Israelachvili, J. Bioinspired Bottle-Brush Polymer Exhibits Low Friction and Amontons-like Behavior. *J. Am. Chem. Soc.* **2014**, *136* (17), 6199−6202.

(7) Faivre, J.; Shrestha, B. R.; Xie, G.; Delair, T.; David, L.; Matyjaszewski, K.; Banquy, X. Unraveling the Correlations between Conformation, Lubrication, and Chemical Stability of Bottlebrush Polymers at Interfaces. *Biomacromolecules* **2017**, *18* (12), 4002−4010.

(8) Zheng, X.; Zhang, C.; Bai, L.; Liu, S.; Tan, L.; Wang, Y. Antifouling Property of Monothiol-Terminated Bottle-Brush Poly-(Methylacrylic Acid)- Graft -Poly(2-Methyl-2-Oxazoline) Copolymer on Gold Surfaces. *J. Mater. Chem. B* **2015**, *3* (9), 1921−1930.

(9) Gao, Q.; Yu, M.; Su, Y.; Xie, M.; Zhao, X.; Li, P.; Ma, P. X. Rationally Designed Dual Functional Block Copolymers for Bottlebrush-like Coatings: In Vitro and in Vivo Antimicrobial, Antibiofilm, and Antifouling Properties. *Acta Biomater.* **2017**, *51*, 112−124.

(10) Pesek, S. L.; Lin, Y.-H.; Mah, H. Z.; Kasper, W.; Chen, B.; Rohde, B. J.; Robertson, M. L.; Stein, G. E.; Verduzco, R. Synthesis of Bottlebrush Copolymers Based on Poly(Dimethylsiloxane) for Surface Active Additives. *Polymer* **2016**, *98*, 495−504.

(11) Xu, Y.; Wang, W.; Wang, Y.; Zhu, J.; Uhrig, D.; Lu, X.; Keum, J. K.; Mays, J. W.; Hong, K. Fluorinated Bottlebrush Polymers Based on Poly(Trifluoroethyl Methacrylate): Synthesis and Characterization. *Polym. Chem.* **2016**, *7* (3), 680−688.

(12) Lepage, M. L.; Simhadri, C.; Liu, C.; Takaffoli, M.; Bi, L.; Crawford, B.; Milani, A. S.; Wulff, J. E. A Broadly Applicable Cross-Linker for Aliphatic Polymers Containing C−H Bonds. *Science* **2019**, *366* (6467), 875−878.

(13) Wang, Y.; An, Q.; Zhou, Y.; Niu, Y.; Akram, R.; Zhang, Y.; Shi, F. Post-Infiltration and Subsequent Photo-Crosslinking Strategy for Layer-by-Layer Fabrication of Stable Dendrimers Enabling Repeated Loading and Release of Hydrophobic Molecules. *J. Mater. Chem. B* **2015**, *3* (4), 562−569.

(14) Yuan, R.; Kopeć, M.; Xie, G.; Gottlieb, E.; Mohin, J. W.; Wang, Z.; Lamson, M.; Kowalewski, T.; Matyjaszewski, K. Mesoporous Nitrogen-Doped Carbons from PAN-Based Molecular Bottlebrushes. *Polymer* **2017**, *126*, 352−359.

(15) Slegeris, R.; Ondrusek, B. A.; Chung, H. Catechol- and Ketone-Containing Multifunctional Bottlebrush Polymers for Oxime Ligation and Hydrogel Formation. *Polym. Chem.* **2017**, *8* (32), 4707−4715.

(16) Gopinadhan, M.; Deshmukh, P.; Choo, Y.; Majewski, P. W.; Bakajin, O.; Elimelech, M.; Kasi, R. M.; Osuji, C. O. Thermally Switchable Aligned Nanopores by Magnetic-Field Directed Self-Assembly of Block Copolymers. *Adv. Mater.* **2014**, *26* (30), 5148−5154.

(17) Mahajan, L. H.; Ndaya, D.; Deshmukh, P.; Peng, X.; Gopinadhan, M.; Osuji, C. O.; Kasi, R. M. Optically Active Elastomers from Liquid Crystalline Comb Copolymers with Dual Physical and Chemical Cross-Links. *Macromolecules* **2017**, *50* (15), 5929−5939.

(18) Ndaya, D.; Bosire, R.; Mahajan, L.; Huh, S.; Kasi, R. Synthesis of Ordered, Functional, Robust Nanoporous Membranes from Liquid Crystalline Brush-like Triblock Copolymers. *Polym. Chem.* **2018**, *9* (12), 1404−1411.

(19) Deshmukh, P.; Gopinadhan, M.; Choo, Y.; Ahn, S.; Majewski, P. W.; Yoon, S. Y.; Bakajin, O.; Elimelech, M.; Osuji, C. O.; Kasi, R. M. Molecular Design of Liquid Crystalline Brush-Like Block Copolymers for Magnetic Field Directed Self-Assembly: A Platform for Functional Materials. *ACS Macro Lett.* **2014**, *3* (5), 462−466.

(20) Reynolds, V. G.; Mukherjee, S.; Xie, R.; Levi, A. E.; Atassi, A.; Uchiyama, T.; Wang, H.; Chabinyc, M. L.; Bates, C. M. Super-Soft Solvent-Free Bottlebrush Elastomers for Touch Sensing. *Mater. Horiz.* **2020**, *7* (1), 181−187.

(21) Mukherjee, S.; Xie, R.; Reynolds, V. G.; Uchiyama, T.; Levi, A. E.; Valois, E.; Wang, H.; Chabinyc, M. L.; Bates, C. M. Universal Approach to Photo-Crosslink Bottlebrush Polymers. *Macromolecules* **2020**, *53*, 1090.

(22) Mah, A. H.; Mei, H.; Basu, P.; Laws, T. S.; Ruchhoeft, P.; Verduzco, R.; Stein, G. E. Swelling Responses of Surface-Attached Bottlebrush Polymer Networks. *Soft Matter* **2018**, *14* (32), 6728−6736.

(23) Liberman-Martin, A. L.; Chu, C. K.; Grubbs, R. H. Application of Bottlebrush Block Copolymers as Photonic Crystals. *Macromol. Rapid Commun.* **2017**, *38* (13), 1700058.

(24) Hu, M.; Xia, Y.; McKenna, G. B.; Kornfield, J. A.; Grubbs, R. H. Linear Rheological Response of a Series of Densely Branched Brush Polymers. *Macromolecules* **2011**, *44* (17), 6935−6943.

(25) van Hensbergen, J. A.; Burford, R. P.; Lowe, A. B. Post-functionalization of a ROMP Polymer Backbone via Radical Thiol-ene Coupling Chemistry. *J. Polym. Sci., Part A: Polym. Chem.* **2013**, *51* (3), 487−492.

(26) Griesser, T.; Wolfberger, A.; Daschiel, U.; Schmidt, V.; Fian, A.; Jerrar, A.; Teichert, C.; Kern, W. Cross-Linking of ROMP Derived Polymers Using the Two- Photon Induced Thiol − Ene Reaction: Towards the Fabrication of 3D-Polymer Microstructures. *Polym. Chem.* **2013**, *4* (5), 1708−1714.

(27) Zhang, K.; Lackey, M. A.; Cui, J.; Tew, G. N. Gels Based on Cyclic Polymers. *J. Am. Chem. Soc.* **2011**, *133* (11), 4140−4148.

(28) Wolfberger, A.; Rupp, B.; Kern, W.; Griesser, T.; Slugovc, C. Ring Opening Metathesis Polymerization Derived Polymers as Photoresists: Making Use of Thiol-Ene Chemistry. *Macromol. Rapid Commun.* **2011**, *32* (6), 518−522.

(29) Mitra, I.; Li, X.; Pesek, S. L.; Makarenko, B.; Lokitz, B. S.; Uhrig, D.; Ankner, J. F.; Verduzco, R.; Stein, G. E. Thin Film Phase Behavior of Bottlebrush/Linear Polymer Blends. *Macromolecules* **2014**, *47* (15), 5269−5276.

(30) Li, M.; De, P.; Gondi, S. R.; Sumerlin, B. S. End Group Transformations of RAFT-Generated Polymers with Bismaleimides: Functional Telechelics and Modular Block Copolymers. *J. Polym. Sci., Part A: Polym. Chem.* **2008**, *46* (15), 5093−5100.

(31) Willcock, H.; O'Reilly, R. K. End Group Removal and Modification of RAFT Polymers. *Polym. Chem.* **2010**, *1* (2), 149−157.

(32) Jiang, L.; Nykypanchuk, D.; Ribbe, A. E.; Rzayev, J. One-Shot Synthesis and Melt Self-Assembly of Bottlebrush Copolymers with a Gradient Compositional Profile. *ACS Macro Lett.* **2018**, *7* (6), 619−623.

(33) Le, D.; Morandi, G.; Legoupy, S.; Pascual, S.; Montembault, V.; Fontaine, L. Cyclobutenyl Macromonomers: Synthetic Strategies and Ring-Opening Metathesis Polymerization. *Eur. Polym. J.* **2013**, *49* (5), 972−983.

(34) Xia, Y.; Kornfield, J. A.; Grubbs, R. H. Efficient Synthesis of Narrowly Dispersed Brush Polymers via Living Ring-Opening Metathesis Polymerization of Macromonomers. *Macromolecules* **2009**, *42* (11), 3761−3766.

(35) Mei, H.; Laws, T. S.; Mahalik, J. P.; Li, J.; Mah, A. H.; Terlier, T.; Bonnesen, P.; Uhrig, D.; Kumar, R.; Stein, G. E.; Verduzco, R.

https://dx.doi.org/10.1021/acsmacrolett.0c00384
ACS Macro Lett. 2020, 9, 1135−1142

Entropy and Enthalpy Mediated Segregation of Bottlebrush Copolymers to Interfaces. *Macromolecules* **2019**, *52*, 8910.
(36) Pesek, S. L.; Xiang, Q.; Hammouda, B.; Verduzco, R. Small-Angle Neutron Scattering Analysis of Bottlebrush Backbone and Side Chain Flexibility. *J. Polym. Sci., Part B: Polym. Phys.* **2017**, *55* (1), 104−111.
(37) Li, X.; Prukop, S. L.; Biswal, S. L.; Verduzco, R. Surface Properties of Bottlebrush Polymer Thin Films. *Macromolecules* **2012**, *45* (17), 7118−7127.
(38) Deshmukh, P.; Ahn, S.; Gopinadhan, M.; Osuji, C. O.; Kasi, R. M. Hierarchically Self-Assembled Photonic Materials from Liquid Crystalline Random Brush Copolymers. *Macromolecules* **2013**, *46* (11), 4558−4566.
(39) Palacios, M.; García, O.; Rodríguez-Hernández, J. Constructing Robust and Functional Micropatterns on Polystyrene Surfaces by Using Deep UV Irradiation. *Langmuir* **2013**, *29* (8), 2756−2763.
(40) Grassie, N.; Weir, N. A. The Photooxidation of Polymers. II. Photolysis of Polystyrene. *J. Appl. Polym. Sci.* **1965**, *9* (3), 975−986.
(41) Torikai, A.; Takeuchi, A.; Fueki, K. The Effect of Temperature on the Photo-Degradation of Polystyrene. *Polym. Degrad. Stab.* **1986**, *14* (4), 367−375.
(42) Kuzina, S. I.; Mikhailov, A. I. Photo-Oxidation of Polymers 4. The Dual Mechanism of Polystyrene Photo-Oxidation: A Hydroperoxide and a Photochain One. *Eur. Polym. J.* **2001**, *37* (11), 2319−2325.
(43) Arrington, K. J.; Murray, C. B.; Smith, E. C.; Marand, H.; Matson, J. B. Precision Polyketones by Ring-Opening Metathesis Polymerization: Effects of Regular and Irregular Ketone Spacing. *Macromolecules* **2016**, *49* (10), 3655−3662.
(44) Kuzina, S. I.; Mikhailov, A. I.; Gol'danskii, V. I. Free Radicals on Photolysis and Radiolysis of Polystyrene. *Int. J. Radiat. Phys. Chem.* **1976**, *8* (4), 503−510.
(45) Cramer, N. B.; Bowman, C. N. Kinetics of Thiol−Ene and Thiol−Acrylate Photopolymerizations with Real-Time Fourier Transform Infrared. *J. Polym. Sci., Part A: Polym. Chem.* **2001**, *39* (19), 3311−3319.
(46) Vaselabadi, S. A.; Shakarisaz, D.; Ruchhoeft, P.; Strzalka, J.; Stein, G. E. Radiation Damage in Polymer Films from Grazing-Incidence X-Ray Scattering Measurements. *J. Polym. Sci., Part B: Polym. Phys.* **2016**, *54* (11), 1074−1086.
(47) Han, S.; Kim, C.; Kwon, D. Thermal/Oxidative Degradation and Stabilization of Polyethylene Glycol. *Polymer* **1997**, *38* (2), 317−323.
(48) Rabek, J. F.; Rånby, B. Studies on the Photooxidation Mechanism of Polymers. I. Photolysis and Photooxidation of Polystyrene. *J. Polym. Sci., Polym. Chem. Ed.* **1974**, *12* (2), 273−294.
(49) Yasuda, N.; Wang, Y.; Tsukegi, T.; Shirai, Y.; Nishida, H. Quantitative Evaluation of Photodegradation and Racemization of Poly(l-Lactic Acid) under UV-C Irradiation. *Polym. Degrad. Stab.* **2010**, *95* (7), 1238−1243.
(50) Wochnowski, C.; Shams Eldin, M. A.; Metev, S. UV-Laser-Assisted Degradation of Poly(Methyl Methacrylate). *Polym. Degrad. Stab.* **2005**, *89* (2), 252−264.
(51) Bei, J.; He, W.; Hu, X.; Wang, S. Photodegradation Behavior and Mechanism of Block Copoly(Caprolactone-Ethylene Glycol). *Polym. Degrad. Stab.* **2000**, *67* (2), 375−380.

https://dx.doi.org/10.1021/acsmacrolett.0c00384
ACS Macro Lett. 2020, 9, 1135−1142